Spatial and temporal variability of atmospheric sulfur-containing gases and particles during the Albatross campaign

Jean Sciare, E. Baboukas, Maria Kanakidou, U. Krischke, Sauveur Belviso, H. Bardouki, Nikolaos Mihalopoulos

JOURNAL OF GEOPHYSICAL RESEARCH, VOL. 105, NO. D11, PAGES 14,433–14,448, JUNE 16, 2000

Spatial and temporal variability of atmospheric sulfur-containing gases and particles during the Albatross campaign

J. Sciare,[1] E. Baboukas,[2] M. Kanakidou,[2] U. Krischke,[3] S. Belviso,[1] H. Bardouki,[2] and N. Mihalopoulos[2]

Abstract. To investigate the oxidation chemistry of dimethylsulfide (DMS) in the marine atmosphere, atmospheric DMS, SO_2, as well as several DMS oxidation products in aerosol phase such as non-sea-salt sulfate (nss-SO_4), methanesulfonate (MSA), and dimethylsulfoxide (DMSOp) have been measured during the Albatross campaign in the Atlantic Ocean from October 9 to November 2, 1996. Long-range transport, local sea-to-air flux of DMS (F_{DMS}), marine boundary layer (MBL) height variation, and photochemistry were found to be the major factors controlling atmospheric DMS concentration which ranged from 29 to 396 parts per trillion by volume (pptv) (mean of 120±68 pptv) over the cruise. The spatial variability of MSA and DMSOp follows the latitudinal variations of F_{DMS}. A 2-day period of intensive photochemistry associated with quite stable atmospheric conditions south of the equator allowed the observation of anticorrelated diurnal variations between DMS and its main oxidation products. A chemical box model describing sulfur chemistry in the marine atmosphere was used to reproduce these variations and investigate coherence of experimentally calculated fluxes F_{DMS} with observed DMS atmospheric concentrations. The model results reveal that the measured OH levels are not sufficient to explain the observed DMS daytime variation. Oxidizing species other than OH, probably BrO, must be involved in the oxidation of DMS to reproduce the observed data.

1. Introduction

Many efforts have been made in the last years to understand the processes controlling the formation of particles in the remote marine atmosphere (see, for instance, the First Aerosol Characterization Experiment (ACE 1) [*Bates et al.*, 1998]). Particles play an important climatic role since they can scatter solar radiation and they can act as a cloud condensation nuclei (CCN), thus influencing the Earth's albedo and subsequently climate [Intergovernmental Panel on Climate Change (*IPCC*), 1994]. Atmospheric dimethylsulfide (DMS), through its end-products, is proposed to be the main compound leading to formation of new particles in the remote marine atmosphere [*Charlson et al.*, 1987].

DMS is produced in seawater from the activity of various phytoplanktonic species. Once released in the atmosphere it will follow an oxidation scheme controlled mainly by OH radicals, the main oxidant in the remote marine atmosphere. Halogen and halogen oxides, especially BrO, have been also proposed to play a significant role in the oxidation pathway of DMS in the remote marine atmosphere [*Toumi*, 1994]. Various authors have shown that DMS follows a daytime cycle in the remote marine atmosphere, generally consistent with simulations of photochemical models considering only the OH-initiated reactions of DMS and its sea-to-air flux [*Andreae et al.*, 1985; *Ayers et al.*, 1995]. In parallel, other studies [see, e.g., *Yvon et al.*,1996; *Chin et al.*, 1996] showed that in several cases the amplitude of the measured daytime cycle of DMS is significantly larger than that predicted by a photochemical model in which OH radical is the only oxidant for DMS. Therefore these authors speculated on the possible contribution of radicals other than OH in the oxidation scheme of DMS. However, lack of measurements of BrO and/or even OH radicals in the marine atmosphere does not allow any conclusion to be made on their relative contribution to the oxidation of DMS.

Although several experiments have been performed to identify the parameters controlling the atmospheric DMS concentrations in the marine atmosphere [*Andreae et al.*, 1995; *Ayers et al.*, 1995], very few experiments were performed to study the latitudinal behavior of this compound (both in seawater and the atmosphere) along with its oxidation products (SO_2, dimethylsulfoxyde (DMSO), nss-SO_4, methanesulfonate (MSA)).

Measurements of atmospheric DMS and its oxidation products in gas and particulate phase in conjunction with "in situ" measurements of OH radicals and their latitudinal variation during the Albatross cruise (following the 30°W from 58°N to 42°S) allowed us (1) to study the factors controlling the latitudinal variation of DMS and its oxidation products and (2) to investigate the relative contribution of OH radicals in the oxidation of DMS in the marine atmosphere through modeling studies.

[1]Laboratoire des Sciences du Climat et de l'Environnement, CEA Orme des Merisiers, Gif-sur-Yvette, France.

[2]Evironmental Chemical Processes Laboratory, Department of Chemistry, University of Crete, Heraklion, Greece.

[3]Department of Atmospheric Sciences, University of California, Los Angeles.

Paper number 1999JD901155.
0148-0227/00/1999JD901155$09.00

2. Experiment

The Albatross campaign was conducted aboard of the German ice breaker R/V *Polarstern* from Bremerhaven (Germany) to Punta Quilla (Argentina) from October 5 to November 11, 1996. After leaving Bremerhaven, the ship reached the Arctic circle north of Iceland (October 10), then followed roughly the 30°W longitude southward until 45°S (October 11 to November 3) arrived at the South American coast at 50°S (November 10; Figure 1a). The sampling was conducted along the 30°W (from 60°N to 45°S) thus covering the main parts of North and South Atlantic Ocean. The sampling was performed on the working deck, at the front of the ship around 25 m above sea level, close to the sampling devices of all other participating groups.

2.1. Atmospheric DMS

DMS was collected into 6-L stainless steel electropolished canisters by compressing air up to 5 bars. Time of collection was typically of the order of 10 min, with a mean of one air sample collected every 4 hours during all the reported period. The analysis was conducted immediately after the collection using a gas chromatograph (VARIAN 3400) equipped with a FPD detector as described by *Nguyen et al.* [1990]. Regular DMS calibrations using permeation tubes (wafer-type permeation source, VICI Metronics, Santa Clara, California) were performed through the entire sampling period and did not show any detectable variation in the sensitivity of the detector. Detection limit was typically of the order of 2 ng (DMS) which in our sampling conditions corresponds to approximately 10 pptv of atmospheric DMS. Accuracy of the analysis was of the order of 5%. Comparisons of sampling in canisters with "on-line" sampling have shown differences (± 5.4%) of the same order of magnitude with the accuracy of the analysis. The DMS was found to be stable in the canisters for at least 9 days (change less than 7%). Finally, no destruction of DMS by oxidants during the preconcentration step has been detected by DMS standard additions.

2.2. Atmospheric SO_2

Atmospheric SO_2 samples were collected using annular denuders equipped with a mini impactor (2.1 μm cutoff diameter). The denuders were coated with Na_2CO_3 and positioned approximately 25 m above the sea level on the working deck. More details concerning the denuder sampling system are presented by *Baboukas et al.* [this issue] and *Lawrence and Koutrakis* [1994]. Exposure times varied from 10 to 22 hours. A total of 31 SO_2 samples were thus continuously collected from 62°N to 38°S covering the period from October 11 to November 2, 1996. Following exposure, the denuders were extracted with 10 mL of Milli-Q water, and approximately 50 μL of chloroform were added as a biocide

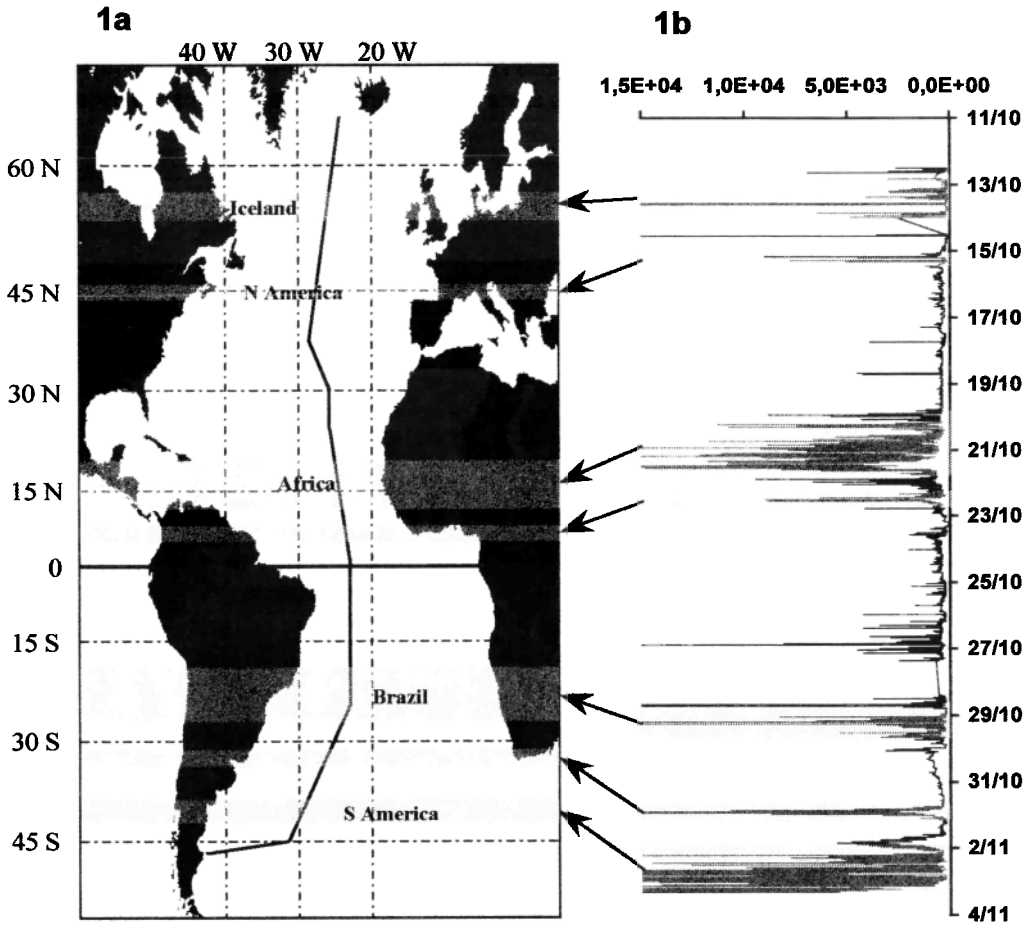

Figure 1. (a) The ship track during the Albatross campaign in the Atlantic Ocean. (b) Condensation nuclei number variation during the cruise. Gray areas correspond to pollution events.

to preserve chemical species against bacterial decomposition. Approximately 10% of the coated denuders were used as field blanks. The blanks have been obtained by exposing the coated denuders to the ambient air for few minutes and subsequently proceeded as for the samples. The extracts were stored in Nalgene opaque polyethylene bottles at +4°C. Analysis was performed by ion chromatography within 3 to 5 weeks after the campaign. SO_2 was detected as sulfate and determined with isocratic elution at 2.0 mL $min^{-1}$of Na_2CO_3/$NaHCO_3$ eluent. Field blank extracts contained nondetectable amounts of SO_4. The method has been calibrated with aqueous standards. The detection limit for SO_2, calculated as the total sulfate (sea salt and nss sulfate) was 3.4 pptv, and the precision was 3% at detection limit.

2.3. Aerosols Collection

Fine aerosol particles (d < 1.1 μm; N=31) were collected on 0.45 μm Gelman Zefluor PTFE filters placed behind the denuder tubes (hereafter mentioned as "Low-vol") operated at a flow of 9 sL min^{-1}. The collection of the fine fraction of the particulate matter was attained by the use of an impactor, placed before the denuder device, with a cutoff diameter of 2.1 μm. In addition, size-segregated aerosols were collected on Whatman-41 filter paper over sampling periods of 12 to 24-hour by means of a six-stage cascade impactor (Sierra-Andersen, Model 230 impactor; hereafter mentioned as "Hi-vol"). The Hi-vol impactor was placed near the denuder system and operated at a flow rate of 85 m^3 h^{-1}. At this flow rate the impactor separated the particles into the following aerodynamic equivalent diameter (Dp) ranges: Stage 1: > 6.40 μm, stage 2: 2.67-6.40 μm, stage 3: 1.33-2.67 μm, stage 4: 0.84-1.33 μm, stage 5: 0.44-0.84 μm. Particles with diameters lower than 0.44 μm were collected on the backup Whatman-41 filter. A total of 29 sets of samples were collected using this cascade impactor from 57°N to 46°S. Filters were prewashed in the laboratory with 0.1 M HCl, rinsed four-five times with Milli-Q water and dried in a clean-air hood. After drying, filters were sealed individually in aluminum foil and polyethylene bags which were opened just before use. At least 5% of washed filters (per batch) were used as laboratory blanks and 5% as field blanks.

Teflon and Whatman-41 filters were extracted by 10 and 20 mL of Milli-Q water respectively, for 45 min in ultrasonic bath. The extraction efficiency with this method was higher than 98% for all compounds of interest. In sample extracts 50-100 μL chloroform were added as a biocide and all the extracts were analyzed within a week using ion-chromatography. Details on the analysis are given at *Baboukas et al.* [this issue]. Precision was 3-6%. For the aerosol phase and the Low-vol sampling, the detection limits, were 2 and 1.2 pptv for sulfate and methanesulfonate respectively. For the Hi-vol setup the detection limits were better than 0.02 pptv for both compounds.

2.4. DMSO Determination in Aerosols

DMSOp determination in aerosols was performed from the Hi-vol impactor filters by extracting them with 50 mL Milli-Q water for 30 min in ultrasonic bath. As detailed by *Sciare et al.* [1998], particular attention has been paid on using "DMSO-free" Milli-Q water for the extraction step. Following the recommendation of *Andreae* [1980], 20 μL of fuming hydrochloric acid (HCl, 37%) were added to the extracts to avoid microbial consumption of DMSO. DMSO was reduced to DMS by $NaBH_4$ and subsequently analyzed using a gas-chromatograph equipped with FPD. The reproducibility, determined by analyzing the same extract 5 times and different parts of the same filter was found to be better than 10%. Tests of conservation on the impacted filters did not show any significant variation of DMSO levels at least over a 6-month period. Preliminary tests of DMSOp stability on the filters performed by parallel sampling of two filters, one with a denuder in front impregnated with Na_2NO_3 to remove the oxidants and another without, did not reveal any significant difference. More details concerning the analysis of DMSO are given by *Sciare and Mihalopoulos* [2000]. The detection limit was better than 1.7 10^{-3} pptv.

2.5. Condensation Nuclei

Measurements of condensation nuclei (CN) were performed during the campaign by the Juelich-KFA group using a 3010 TSI Model with a lower detection limit of 10 nm, and a measuring frequency of a minute. This counter was located also on the working deck.

3. Results and Discussion

3.1. Meteorological Parameters

Meteorological parameters such as wind speed, wind direction, air and seawater temperature and relative humidity (RH) were continuously recorded from the instruments on board the R/V *Polarstern*. The height of MBL was estimated from the daily ozone radio soundings and Lidar measurements performed on board (R. Weller and P. Rairoux, personal communication, 1999). Very good agreement was found between the first aerosol layer height determined by Lidar measurements and the inversion height (in RH, and air temperature) observed by ozone radio soundings and defined here as the MBL height (report to Figure 2a).

To identify the periods of pure marine conditions from those under continental/polluted air masses influence, we reported condensation nuclei measurements as a function of date and in conjunction with the track (Figures 1a and 1b). In conjunction with atmospheric NO, NO_2, black carbon measurements as well as back trajectories, we were able to identify periods under continental/polluted air masses influence (gray areas displayed on the track; Figures 1a and 1b).

3.2. DMS Sea-to-Air Flux F_{DMS} Calculation

DMS concentrations in surface seawater measured during the whole cruise with a resolution of 10-15 km ranged from 0.15 to 6.6 nM. Details on the seawater DMS measurements are given by *Belviso et al.* [this issue]. On the basis of these high spatio-temporal resolution DMS observations in seawater, sea-to-air DMS fluxes were calculated using the following equation described by *Liss and Slater* [1974]:

$$F_{DMS} = K_w C_w$$

where C_w is the DMS concentration in seawater and K_w is the DMS gas-transfer velocity.

The K_w was calculated by using the relationship proposed by *Liss and Merlivat* [1986] relating K_w with wind speed and seawater temperature. Wind speed and seawater temperature were obtained continuously while underway from the equipment available aboard of R/V *Polarstern*.

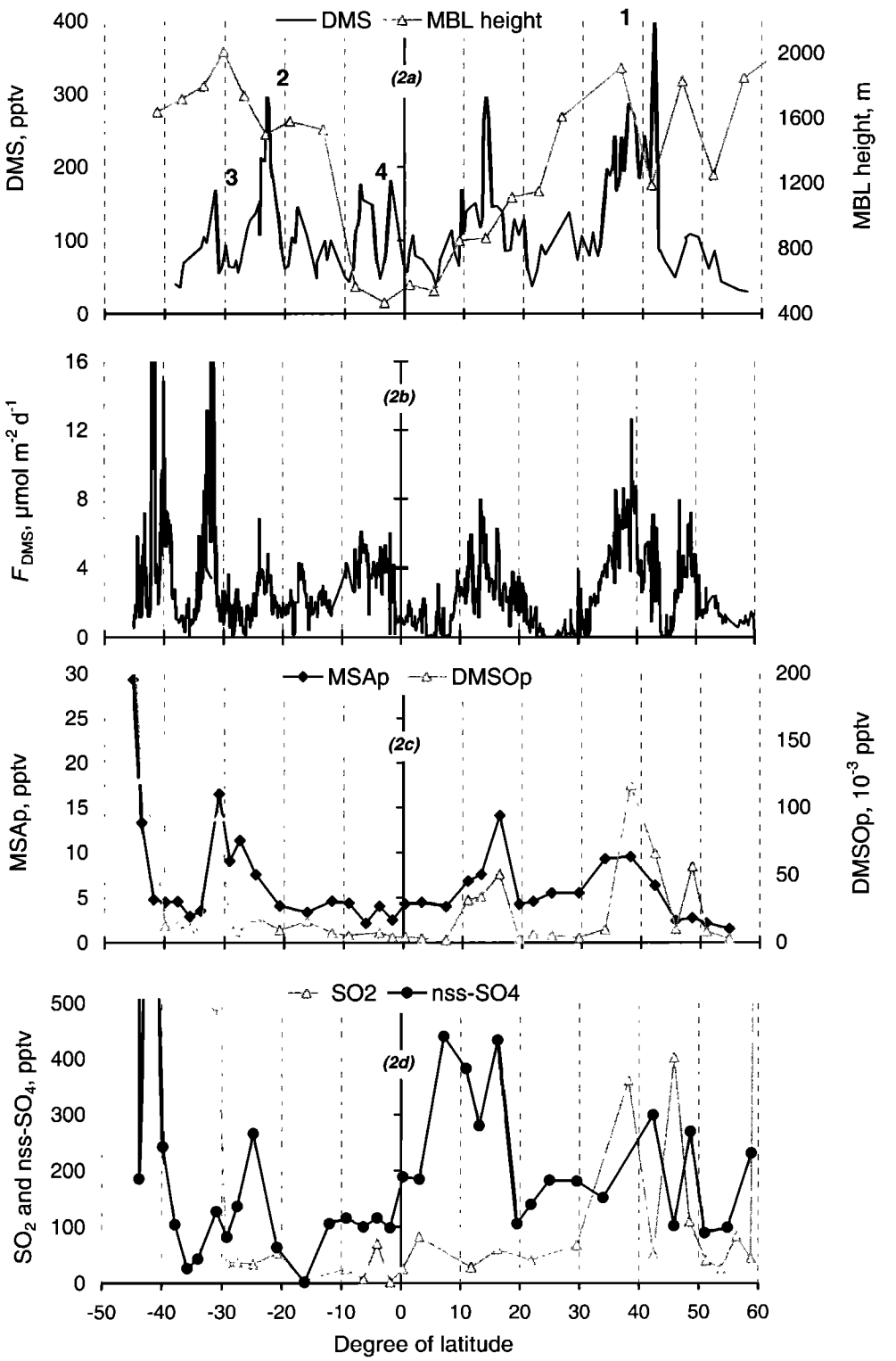

Figure 2. Latitudinal variation of (a) atmospheric DMS and MBL, (b) DMS sea-air fluxes, (c) aerosol MSA and DMSO, and (d) nss-SO_4 and SO_2 during the Albatross cruise.

3.3. Factors Controlling the Distribution of Atmospheric DMS

A total of 130 atmospheric samples was collected and analyzed for DMS during the cruise. DMS concentrations ranged from 29 to 396 pptv (with arithmetic mean of 120± 68 pptv).

Table 1 compares our DMS measurements during the Albatross cruise with those reported in literature for the same area. Our mean DMS concentration of 120 pptv is found to be in relatively good agreement with reported atmospheric DMS observations. For instance, our mean value of 122 pptv measured in the temperate Atlantic Ocean is in excellent agreement with the value reported by *Andreae et al.* [1995] in

Table 1. Sulfur Species Atmospheric Mol Fraction Observed During This Cruise and Compared to Literature Data for the Atlantic Ocean

Location / Period	DMS	SO_2	nss-SO_4	MSA	DMSOp, x 10^{-3}	References
Atlantic 58°N-38°S (Oct.-Nov. 1996)	120 ± 68	41 ± 24	169 ± 110	6.4 ± 5.4	86	this work
58°N-30°N	146 ± 87			4.9	(6-638)	
30°N-20°S	107 ± 53			5.1		
20°S-38°S	122 ± 70			9.8		
Atlantic (same period)						
66°N-0°		18 ± 12 [a]	218			*Krischke et al.* [this issue]
0°-38°S		19 ± 13 [a]	147			
Atlantic 19°S (Feb.-March 1991)						
Subtropical and temperate	132 ± 45		(98-379)	12.4		*Andreae et al.* [1995]
Tropical	44 ± 16					
Atlantic 50°N-50°S (Oct.-Nov. 1990)						
50°N-30°N	31		270	2.9		*Staubes and Georgii* [1993]
30°N-20°S	43		150	3.2		
20°S-50°S	430		240	12.9		
Atlantic tropical NE (Sept.-Oct. 1991)	76	37	347	7.3		*Putaud et al.* [1993]
Atlantic 50°N-50°S (Oct. 1992)	14	350	288	3.6		*Davison et al.* [1996]
Atlantic (Sept.-Oct. 1988)						
0-49°N				6.5 ± 1.6		*Bürgermeister and Georgii* [1991]
0-34°S			144[b]	6.5 ± 1.7		
Barbados			220	5.1		*Galloway et al.* [1993]
Bermuda			597	9.3		*Galloway et al.* [1993]
North Atlantic			903	2.4-29.3	≈ 122	*Watts et al.* [1990]
Tropical Atlantic	122 ± 64					*Andreae et al.* [1985]
Atlantic 45°N-30°N		27 ± 8				*Herman and Jaeschke* [1984]
North Atlantic		88 ± 47				*Nguyen et al.* [1983]
South Atlantic		52 ± 68				

Units are in pptv. The ranges of concentrations are shown in parentheses.

[a] SO_2 background concentration ([SO_2]<100 pptv [see *Krischke et al.*, this issue]).

[b] Only between 17° and 29°S.

the same area. Our mean value of 107 pptv measured in the tropical and subtropical area falls between the 76 and 122 pptv reported by *Putaud et al.* [1993] and *Andreae et al.* [1985], respectively. Changes in F_{DMS} and/or MBL height can account for the about a factor of 2 difference between our measurements and those of *Andreae et al.* [1995] and *Staubes and Georgii* [1993] for the tropical Atlantic Ocean. Indeed, as depicted in Figure 2a, during the Albatross cruise the MBL height around the equator was 500 m, comparable to the values observed in equatorial regions [*Yvon et al.*, 1996; *Bandy et al.*, 1996]. In addition seawater DMS concentrations during the Albatross campaign [*Belviso et al.*, this issue] were about a factor of 2 higher than those of 1.1-1.4 nM reported by *Staubes and Georgii* [1993], suggesting that the experimental conditions were different during these two cruises. This is also reflected on the particulate MSA concentrations which are a factor of 2 higher during the Albatross cruise than during the cruise reported by *Staubes and Georgii* [1993] (Table 1).

As shown in Figure 2a, strong variations in atmospheric DMS were observed along the track. To explain such variability in DMS, the major factors expected to control it, such as its sea-to-air flux, OH diurnal variation, MBL height and air mass origin (back trajectories) available during the campaign, were analyzed. From the DMS and F_{DMS} over the whole cruise, depicted in Figures 2a and 2b, several conclusions can be made:

The DMS variations coincide most of the time with the F_{DMS} variations over the cruise, thus, we can assume that the major parameters controlling atmospheric DMS concentration during this cruise were local (strength of the source (F_{DMS}) influenced by the local wind). However, this covariation is not quantitative. When F_{DMS} is plotted as a function of DMS (Figure 3), the correlation coefficient r^2 for a linear regression is weak (0.28). Even if the two apparent "outliers" are removed the r^2 remains weak (0.36). We can thus assume that sea-air exchange of DMS can account for only one third of the observed variability in the atmospheric DMS concentration.

To understand such low accordance, we chose the two "outliers" of the Figure 3, as a case study. The first corresponds to an event occurred at 42°N and is associated with

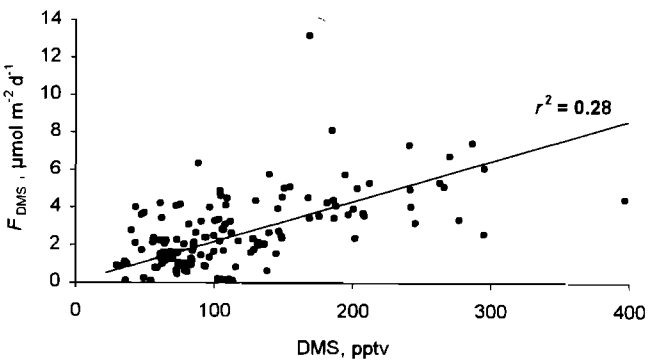

Figure 3. Regression between DMS sea-to-air flux and atmospheric DMS during the Albatross cruise.

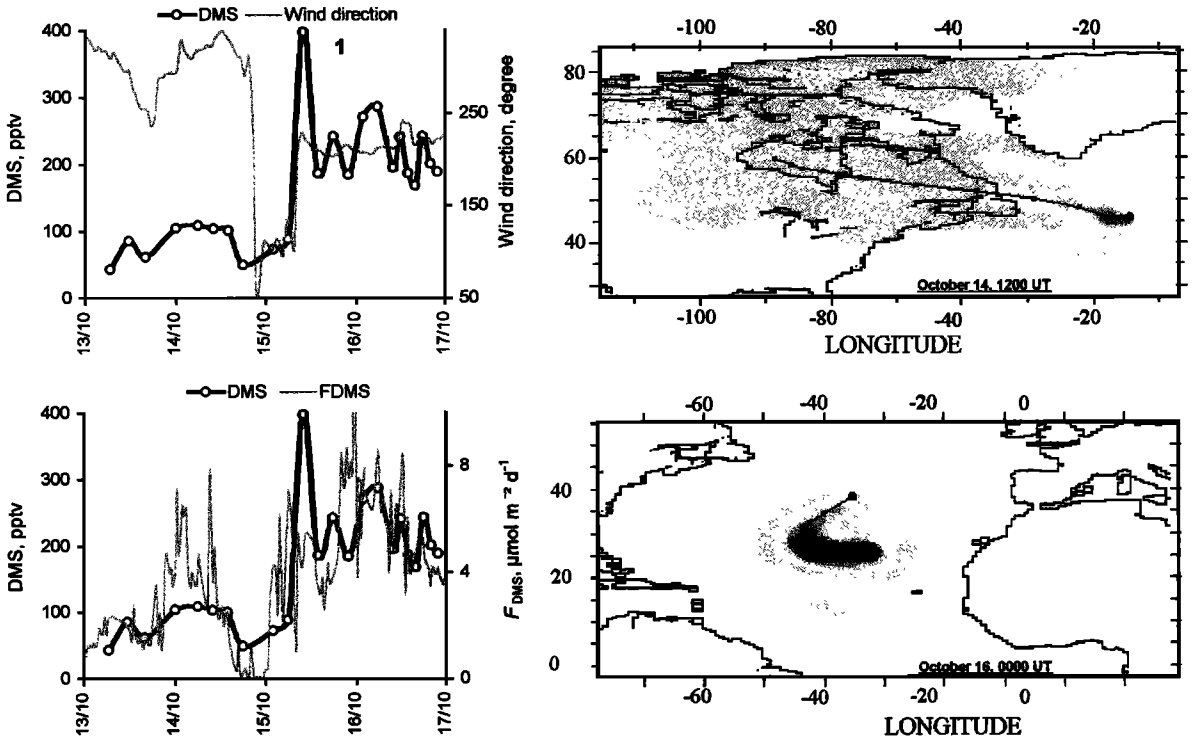

Figure 4a. Atmospheric DMS, sea-air flux, wind direction, and 5-day back trajectory analysis for the period October 13-17, 1996.The shaded areas in the trajectory plots correspond to the region from which the air mass originates. Darker areas show higher probability than lighter areas. The continuous line corresponds to the center of gravity of the air mass calculated every 12 hours.

an increase in DMS by more than 300 pptv (from 89 to 397 pptv) within at least 4 hours (event marked by '1' in Figure 2a). The decrease of the MBL height by 40% observed on October 14-15, is not sufficient to explain such increase in DMS. On the basis of 5-day back trajectory analysis and the local wind direction, this event could be partly explained by a change in the origin of air masses reaching the ship as illustrated in Figure 4a. As displayed in this figure, changes both in the wind direction and the air mass origin (as shown by the 5-day back trajectories) provided pure southerly marine conditions on October 15 after an event of continental air masses from North America occurring on October 14. Changes in source strength and/or oxidation lifetime of DMS (lower in continental air masses due to elevated NO_3 levels) can account for this difference. Similar change in air masses was also observed during an event (marked by '2' in Figure 2a) occurring on October 29, around 24°S and was associated with a decrease in DMS by nearly 200 pptv (from 295 to 108 pptv) within 8 hours (Figure 4b).

The second "outlier" corresponds to an event occurred around 31.5°S (event marked by '3' in Figure 2a). Figure 4b depicts the origin of the sampled air-mass during this event. Although the local DMS flux reached values up to 15 µmol m^{-2} d^{-1}, DMS concentrations remained low. Long-range transport from "low productive DMS areas" of the southern ocean can account for this situation. The enhancement of the MSA/nss-SO_4 ratio occurred during this event (13%, i.e., the highest value observed during the whole cruise) is an additional indication of important influence from colder areas. All the above cases indicate that transport can also significantly influence atmospheric DMS concentrations.

The last interesting situation (event marked by '4' in Figure 2a) was observed during a 2-day period between roughly 0° and 10°S. During this period important day-to-day DMS changes occurred without any significant change in DMS flux, air masses origin and/or MBL height. At these latitudes, photochemistry could be responsible for the observed DMS daytime variations. This period will be discussed in more details in section 3.6 to highlight the diurnal variation of DMS and its oxidation products.

3.4. Atmospheric SO_2

Atmospheric SO_2 concentrations were determined during the campaign using the annular denuder technique and the results are displayed in Figure 2d. High values of SO_2 have been recorded during the cruise at the latitude bands 55-60°N, 45-35°N and below 30°S. These values are associated with high CN values (Figure 1b) and denote continental influence. Except these strong events with SO_2 up to 300 pptv, the recorded atmospheric SO_2 concentrations (average 41 ± 24 pptv) were of the order of those reported for clean marine atmosphere (*de Bruyn et al.* [1998] and *Ayers et al.* [1997] for southern Pacific and references in Table 1 for Atlantic). SO_2 has been also measured during this cruise by means of a filter technique using an aqueous solution of tetrachloromercurate (II) as absorbents [*Krischke et al.*, this issue]. Unfortunately, no quantitative comparison can be performed between these two data sets for two reasons: First, the sampling strategy and sampling step were different: (1) 45 min sampling and no samples during most of the nights by *Krischke et al.* [this issue], (2) 12-22 hours and continuous sampling (this work). Second, the mean value reported by *Krischke et al.* [this

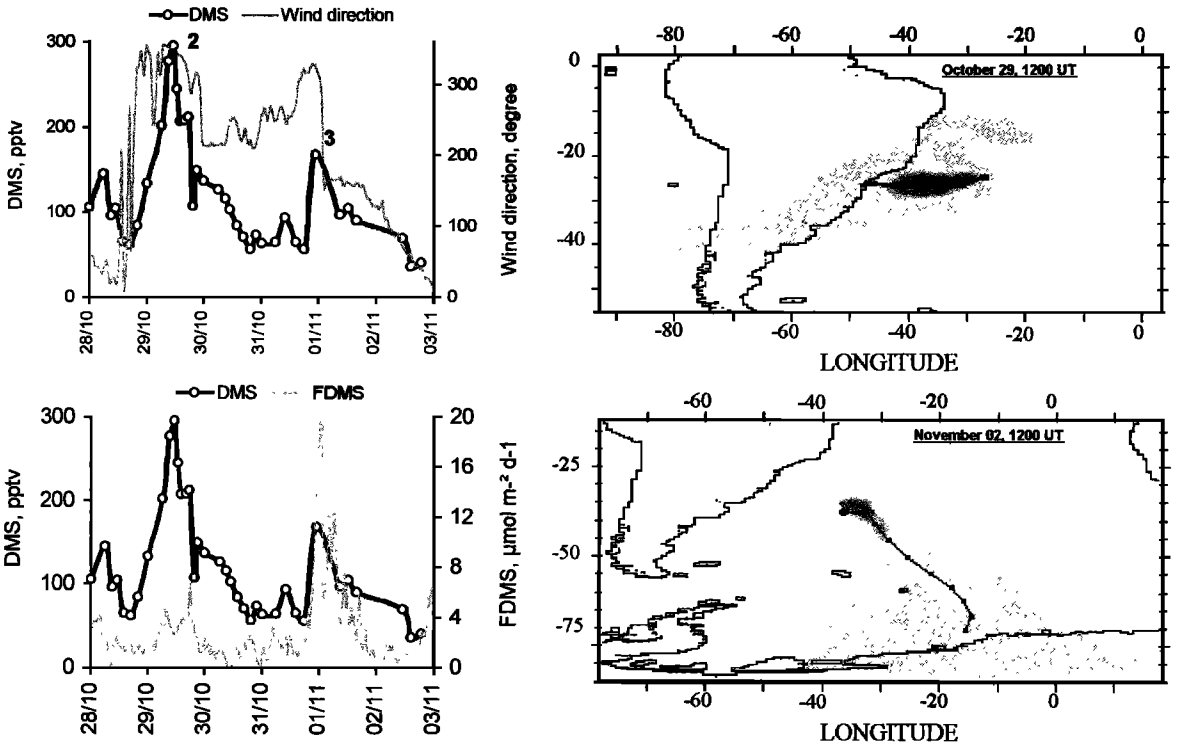

Figure 4b. Atmospheric DMS, sea-air flux, wind direction and 5-day back trajectory analysis for the period October 28 to November 3, 1996 (see explanation of Figure 4a).

issue] excludes concentrations higher than 98 pptv as they could be influenced by anthropogenic sources through long-range transport. Our integrated continuous sampling can not allow elimination of short-term events (few hours) with concentrations above 100 pptv (and less than about 1 ppbv) which certainly influence our mean values. These reasons could account for the "apparent" difference of about a factor of 2 between the two data sets shown in Table 1. Therefore our mean SO_2 values agree reasonably with those reported by *Krischke et al.* [this issue; Table 1]. In the following discussion, we will use the SO_2 data set collected by *Krischke et al.* [this issue] which has the best time resolution.

3.5. Sulfur-Containing Atmospheric Aerosols

3.5.1. The nss-SO_4. The measurements of total nss-SO_4 (sum of the six stages of the cascade impactor) during the Albatross campaign are reported in Table 1 and compared to observations reported in literature. Our mean value of 169 pptv ± 110 observed during the experiment is in good agreement with the mean values of 147 and 218 pptv reported by *Krischke et al.* [this issue] for the southern and northern hemisphere respectively. The particulate nss-SO_4 measured during the Albatross campaign is among the lowest recorded over the Atlantic Ocean, suggesting, in agreement with previous observations on atmospheric SO_2, that pure marine conditions occurred during the major part of the cruise.

The size fractionation of nss-SO_4 in 6 different segregated stages is reported in Figure 5a. Nss-SO_4 is mainly distributed in the fine mode (diameters smaller than 1.3 µm; i.e., stages 4 to 6) since this mode accounts for about 70% of the total nss-SO_4 concentration. *Krischke et al.* [this issue] by using an impactor for separation in two aerosol classes, reported partition of nss-SO_4 in the fine mode (<1.0 µm) of the order of 64%, in very good agreement with our observations. The origin of nss-SO_4 in the coarse mode can be explained by absorption of SO_2 on the basic particles (mainly sea salt). On the other hand, the nss-SO_4 presence in the fine mode is probably due to gas-to-particle conversion.

3.5.2. MSA. MSA measured on the back filters of the denuders (particles with diameters smaller than 2.1 µm) agreed quite well in absolute terms with the MSA collected on the two last stages of the cascade impactor, particles with diameters smaller than 0.84 µm. This indicates a good agreement between these two aerosol sampling devices. Total particulate MSA (MSAp) concentrations, sum of the six stages of the cascade impactor, as given in Table 1, ranged from 0.73 to 29.3 pptv (mean = 6.4 ± 5.4 pptv) and agree well with previous observations. The general trend of MSAp over the cruise (Figure 2c) was found to follow the F_{DMS} (Figure 2b) with its maximum south of 40°S, which was consistent with the previous observations in this area [*Staubes and Georgii*, 1993; *Davison et al.*, 1996].

The size fractionation of MSA in six different segregated stages is depicted in Figure 5b. The fine mode (diameters smaller than 1.3 µm; i.e., stages four to six) accounts for about 71% of the total MSA concentration. A significant part of MSA does exist in the 4th stage compared to nss-SO_4, indicating a more significant adsorption of MSA onto preexisting particles.

3.5.3. Aerosol MSA/nss-SO_4 ratio. Several studies investigated the factors controlling the MSA/nss-SO_4 ratio variability [*Bates et al.*, 1992; *Ayers et al.*, 1996, and references therein] and reported a negative temperature dependence. In order to study such dependencies, MSA/nss-SO_4 ratios have been calculated from the cascade impactor

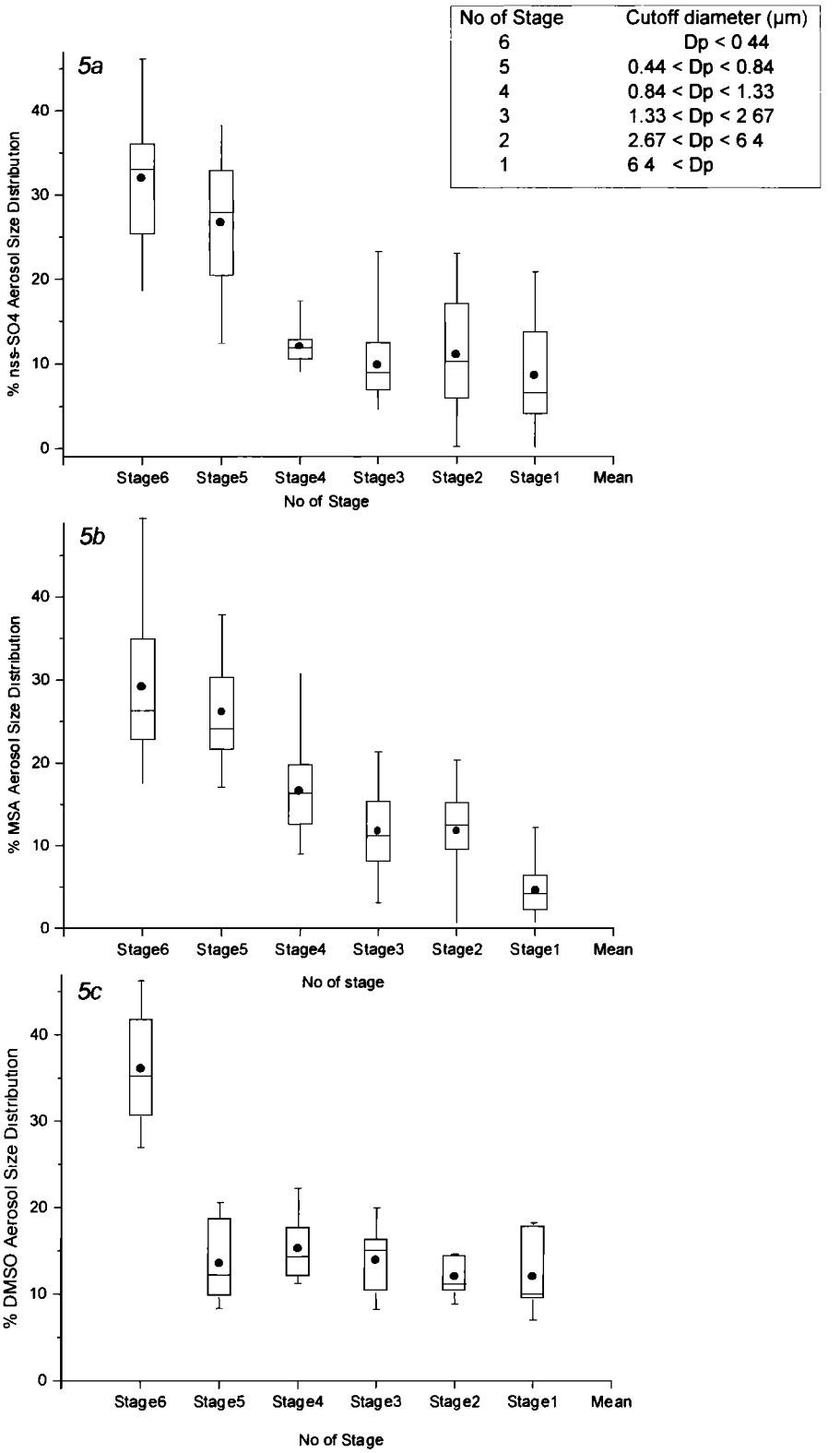

Figure 5. Size fractionation of (a) nss-SO_4, (b) MSA, and (c) DMSO as a function of diameter during the cruise. The box plots contain the 10^{th}, 25^{th}, 50^{th}, 75^{th} and 90^{th} percentiles. The square inside the box plots corresponds to the mean value.

data along the track during periods of background marine conditions as indicated by the 5-day back trajectories. High values ranging between 0.08 and 0.12 (mean 0.10 ± 0.02) were recorded in the temperate south Atlantic (27-36°S), whereas low values ranging between 0.019 and 0.044 (mean 0.028 ± 0.009) was found in the equatorial Atlantic (20°N-20°S). Such observations are in agreement with the work of *Bates et al.*, [1992] also reported a strong latitudinal dependence in this ratio. Our mean value of 0.028 reported for the equatorial Atlantic is in good agreement with the value

derived from *Bates et al.* [1992] equation and observations at the same area [*Putaud et al.*, 1993]. For the temperate Atlantic our mean value of 0.10 is lower compared to the value derived from *Bates et al.* [1992] equation. Anthropogenic influence on the nss-SO_4 concentrations can account for this low values. Indeed, despite the fact that air masses back trajectories indicate pristine marine conditions, isotopic sulfur analysis performed by *Patris et al.* [this issue] indicate a nonnegligible anthropogenic component at this area (around 30%).

3.5.4. DMSOp. Particulate DMSO (DMSOp) measurements were performed on the back up filter of the cascade impactor (aerodynamic equivalent diameter <0.44 μm) with concentrations ranging from 2.2 x 10^{-3} to 211 x 10^{-3} pptv (mean = 32.10^{-3} ± 49.10^{-3} pptv). All the DMSOp determinations for the last stage of the cascade impactor were reported in Figure 2c and similarly to MSAp, were found to be in good accordance with F_{DMS}, with the highest values (211.10^{-3} pptv) recorded south of 40°S. However the stronger variability of DMSOp (maximum differences of a factor of 100) when compared to the MSAp variability (maximum differences of a factor of 20) could be explained by a shorter lifetime of DMSOp compared to MSA in the aerosol phase.

From a first approach, such good agreement between DMSOp and F_{DMS} parameters could suggest that DMSOp in particles sized less than 0.44 μm is produced from local sources of DMS and has a relatively short lifetime. Such behavior cannot nevertheless be attributed to the whole cruise since very low DMSOp values were found around the equator, whereas DMS and F_{DMS} did not present such pattern. Several parameters such as atmospheric DMSO production, gas-to-particle conversion and DMSO stability in the aerosol phase may influence the concentration of DMSOp. The latitudinal dependence of these parameters is discussed below.

1. Strongly dependent on atmospheric temperature, the addition reaction of OH on DMS leading to DMSO production is favored at low temperatures [*Hynes and Wine*, 1996]. Thus, gas phase DMSO formation is expected to be enhanced at the highest latitudes.

2. In addition, as suggested by *Davis et al.* [1998], gas phase DMSO has a longer lifetime with respect to OH reaction at high than at low latitudes. Therefore, gas-to-particle conversion of atmospheric DMSO could represent its major sink at high latitudes.

Indeed during Albatross campaign, the highest DMSOp levels were found at the highest latitudes. Even higher DMSOp concentrations (up to 4.9 pptv) have been observed at higher latitudes at a coastal site in Antarctica (J. Sciare, unpublished data, 1999), supporting the previous analysis.

DMSOp analysis in six complete sets of six-stage impactor fractions revealed that 36.1% ± 6.7 of the collected DMSOp was in the final filter (Figure 5c). No significant difference in DMSOp levels has been observed between the other stages. DMSO has been detected in seawater, at levels that sometimes exceed those of DMS [*Andreae*, 1980; *Kieber et al.*, 1996; *Simo et al.*, 1997]. The low DMSOp partition observed at stages 1-2 indicates that sea spray is not an important source of aerosol DMSO. Thus gas-to-particle conversion seems to be the main process governing the DMSOp formation.

Given the small standard deviation of the mean of DMSOp in the final filter, the total DMSOp concentration in the remaining 25 cascade impactor filters was calculated using the above average (36.1% ± 6.7) and the corresponding DMSOp value in the final filter. DMSOp total concentrations, thus calculated, ranged from (6-638) x 10^{-3} pptv (mean of 86 x 10^{-3} pptv). Our mean total DMSOp is in good agreement with the only DMSOp measurements ever reported in literature (Table 1).

An enhancement in DMSOp production compared to MSA as a function of latitude was observed during the campaign with higher DMSOp/MSA ratio values at high latitudes than at lower latitudes. Indeed the DMSOp/MSA ratio increases from $3.4.10^{-3}$ in the equatorial Atlantic (20°N-20°S) to $10.5.10^{-3}$ in the temperate south Atlantic (27-36°S); that is a factor of 3, comparable to the enhancement of MSA relative to nss-SO_4 (3.5; see paragraph 3.5.3). Such enhancement in the DMSOp/MSA ratio at low temperatures has been also observed in rainwater collected at Amsterdam Island during a 2-year period *Sciare et al.* [1998]. Although the behavior of DMSOp (enhancement at low temperatures) is in line with the previous discussion, further studies are required to elucidate its fate in the particulate phase.

3.6. Photochemical Processes Controlling the DMS Oxidation Scheme: Comparison With a Simple 0-D Chemical Model Simulation

3.6.1. Observations. Owing to unstable weather conditions (change in wind speed and direction, MBL height, insolation), no clear diurnal variations for atmospheric DMS were observed during the track, except for a 2-day period (October 25-26, roughly between 0° and 10°S) when clean marine air (report to Figure 1) and quite stable weather conditions (insolation and wind speed) occurred. MBL height observed in this tropical area (October 23-26) remained quite stable and averaged 539 ± 49m. Owing to stable wind speed and DMS seawater concentrations, F_{DMS} remained also quite stable during these days and averaged 4.0 ± 0.9 μmol m^{-2} d^{-1}.

As depicted in Figure 6a, atmospheric DMS exhibits during these 2 days clear diurnal variations with a maximum of around 175 pptv in the early morning (0800 local time, around 1 hour after the sunrise) and minimum of around 45 pptv in the late afternoon (1700 local time, around 1 hour before the sunset). To examine whether DMS flux variations can account for the observed atmospheric DMS trend, F_{DMS} was plotted as a function of DMS for the reported period (not shown) and the resulting correlation coefficient r^2 for a linear regression was almost 0 (r^2=0.016). Atmospheric SO_2 derived from the high frequency sampling of *Krischke et al.* [this issue], also reported in Figure 6a, shows as well clear diurnal variation, opposite in phase to the DMS pattern. These daytime variations are in line with the results reported by *Bandy et al.* [1996] and *Yvon and Saltzman* [1996] for equatorial and tropical Pacific Ocean respectively. MSA and nss-SO_4 in aerosol phase, follow the same diurnal trend as SO_2 and opposite in phase with that of DMS (Figure 6b). Such patterns are in agreement with the results reported for the same latitudes in the Pacific Ocean by *Huebert et al.* [1996]. Figure 6c presents the variation of condensation nuclei (CN) as well as the opposite of relative humidity (100 - RH) during the same period. CN follows quite well the variation of all DMS oxidation products, but is found also to be very sensitive to RH variation. Similar trend between CN and RH has been reported during ACE 1 experiment [*Bates et*

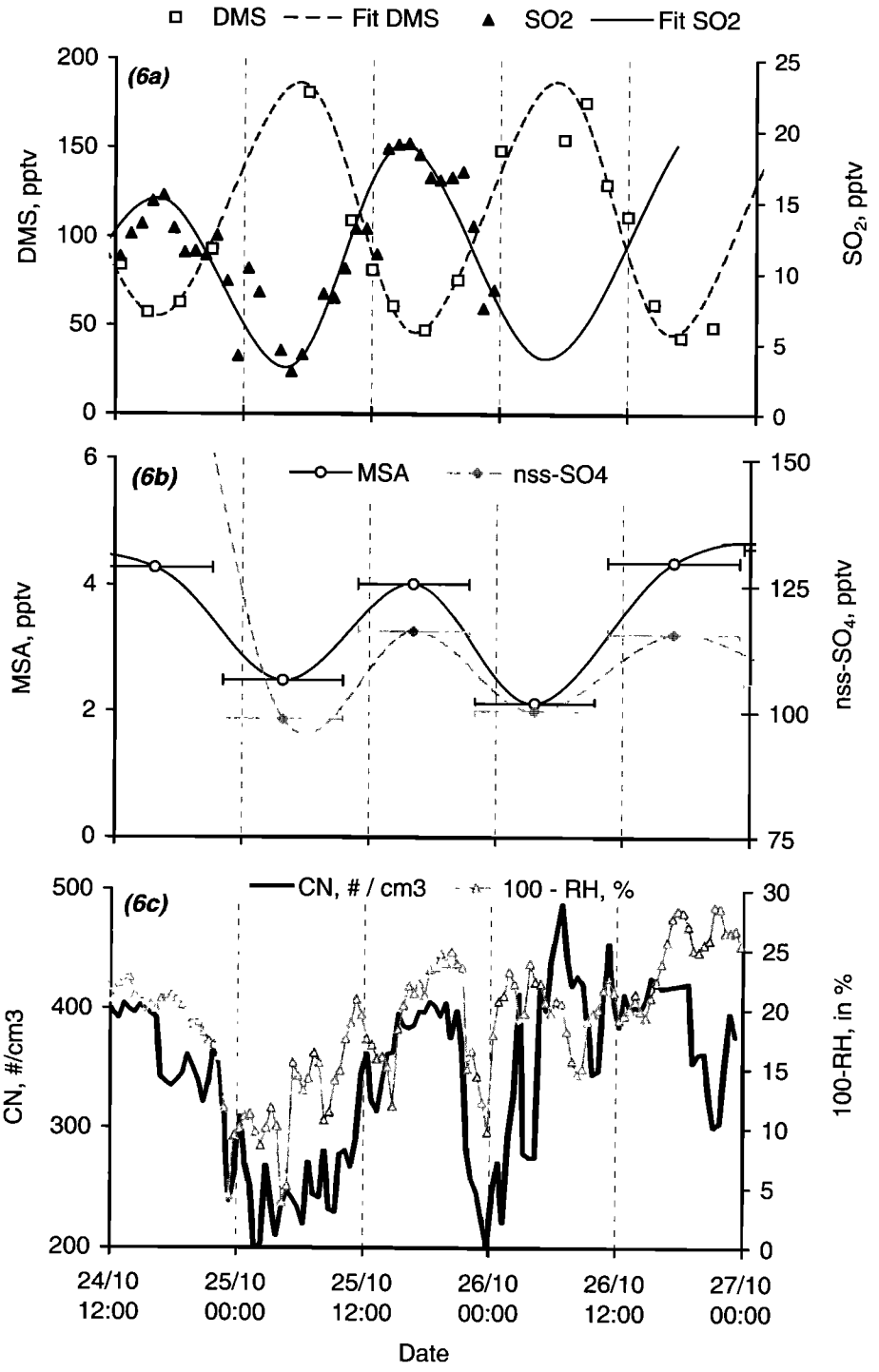

Figure 6. Diurnal variation of (a) atmospheric DMS and SO_2, (b) particulate MSA and nss-SO_4 , and (c) CN and relative humidity between October 25-26, 1996 during the Albatross cruise.

al., 1998]. Despite the apparent sensitivity of CN and RH and the apparent covariation CN - DMS oxidation products, the lack of physical characterisation of aerosols as well as the low frequency of our measurements of the DMS oxidation products do not allow any quantitative relationship between CN variations and DMS oxidation chemistry.

3.6.2. Chemical box model description. To analyze and improve our understanding on the photochemical processes controlling DMS oxidation during this 2-day period, we used a chemical box model. The commercially available software FACSIMILE [*Curtis and Sweetenham*, 1988], which uses automatic time step selection and error control, was used to solve the differential equations with a high accuracy required for chemistry studies. The chemistry model is a condensed chemical mechanism, which, in addition to the background $O_3/NO_x/OH/CO$ and CH_4 chemistry, also takes into account

Table 2. Reactions and Corresponding Rates Used to Describe DMS Oxidation Chemistry in the Chemical Box Model

	Reaction	Rate	Reference
	H Abstraction		
RS1	$DMS + OH \rightarrow CH_3SCH_2 + H_2O$	1.13E-11[a] x exp(-253/*T*)	JPL97
RS2	$CH_3SCH_2 + O_2 \rightarrow CH_3SCH_2O_2$	7.3E-13	YIN
RS3	$CH_3SCH_2O_2 + NO \rightarrow CH_3SCH_2O + NO_2$	8.E-12	YIN
RS4	$CH_3SCH_2O \rightarrow CH_3S + HCHO$	1.E+	YIN
	OH Addition		
RS5	$DMS + OH \rightarrow DMSOH$		(1)
RS6	$DMSOH + O_2 \rightarrow DMSO + HO_2$	2.E-12	KT96
RS7	$DMSOH + O_2 \rightarrow CH_3SOH + CH_3O_2$	1.E-12	KT96
RS8	$DMSOH + O_2 \rightarrow DMSOHO_2$	1.E-12	KT96
	BrO Reaction With DMS[b]		
RS9	$DMS + BRO \rightarrow$ product	4.4E-13	CRO99
	$CH_3S(OH)(OO)CH_3$ Chemistry		
RS10	$CH_3S(OH)(OO)CH_3 + O_2 \rightarrow DMSO_2 + HO_2$	1.2E-12	CP 97
	DMSO Chemistry		
RS11	$DMSO + OH \rightarrow CH_3SO_2H + CH_3O_2$	8.7E-11	HYN
	CH_3SO_2H Chemistry		
RS12	$CH_3SO_2H + OH \rightarrow CH_3SO_2 + H_2O$	1.6E-11	CP 97
RS13	$CH_3SO_2H + NO_3 \rightarrow CH_3SO_2 + H_2O$	1.0E-13	CP 97
RS14	$CH_3SO_2H + HO_2 \rightarrow CH_3SO_2 + HNO_3$	1.0E-15	CP 97
ROHMS3	$CH_3SO_2H + CH_3O_2 \rightarrow CH_3SO_2 + CH_3OOH$	1.0E-15	CP 97
	CH_3SOH Chemistry		
RS15	$CH_3SOH + OH \rightarrow CH_3SO + H_2O$	1.1E-10	YIN
RS16	$CH_3SOH + NO_3 \rightarrow CH_3SO + HNO_3$	3.4E-12	YIN
RS17	$CH_3SOH + HO_2 \rightarrow CH_3SO + H_2O_2$	8.5E-13	YIN
RS18	$CH_3SOH + CH_3O_2 \rightarrow CH_3SO_2 + CH_3OOH$	8.5E-13	YIN
	CH_3S Chemistry		
RS19	$CH_3S + O_2 \rightarrow CH_3SOO$	5.8E-17	YIN
RS20	$CH_3SOO \rightarrow CH_3S + O_2$	6.E+2	YIN
RS21	$CH_3SOO + HO_2 \rightarrow CH_3SO_2H + O_2$	4.E-12	YIN
RS22	$CH_3SOO + CH_3O_2 \rightarrow CH_3SO + HCHO + HO_2$	5.5E-12	YIN
RS23	$CH_3S + NO_2 \rightarrow CH_3SO + NO$	6.1E-11	YIN
	CH_3SO Chemistry		
RS24	$CH_3SO \rightarrow SO + CH_3O_2$	2.7E+32 x exp(-0.1/0.0019872/*T*)	YIN
RS25	$CH_3SO + O_2 \rightarrow CH_3SOOO$	7.7E-18	YIN
RS26	$CH_3SOOO \rightarrow CH_3SO + O_2$	1.7E+2	YIN
RS27	$CH_3SOOO + HO_2 \rightarrow CH_3SOO2H + O_2$	3.E-12	YIN
RS28	$CH_3SOOO + CH_3O_2 \rightarrow CH_3SO_2 + CH_3O + O_2$	5.5E-12	YIN
RS29	$CH_3SO + NO_2 \rightarrow CH_3SO_2 + NO$	3.E-12	YIN
RS30	$CH_3SO + O_3 \rightarrow CH_3SO_2 + O_2$	2.E-12	YIN
	CH_3SO_2 Chemistry		
RS31	$CH_3SO_2 \rightarrow CH_3O_2 + SO_2$	2.6E11 x exp(-9056/ *T*)	AYE
RS32	$CH_3SO_2 + O_2 \rightarrow CH_3SO_2O_2$	2.6E-18	YIN
RS33	$CH_3SO_2O_2 \rightarrow CH_3SO2 + O_2$	3.3	YIN
RS34	$CH_3SO_2 + NO_2 \rightarrow CH_3SO_3 + NO$	1.E-14	YIN
RS35	$CH_3SO_2 + O_3 \rightarrow CH_3SO_3 + O_2$	5.E-15	YIN
RS36	$CH_3SO_2 + HO_2 \rightarrow CH_3SO_3 + OH$	2.5E-13	YIN
	CH_3SO_3 Chemistry		
RS37	$CH_3SO_2 + CH_3O_2 \rightarrow CH_3SO_3 + HCHO + HO_2$	2.5E-13	YIN
RS38	$CH_3S + O_3 \rightarrow CH_3SO + O_2$	6.E-12	YIN
RS39	$CH_3SO_3 \rightarrow SO_3 + CH_3O_2$	1.1E17 x exp(-12057/ *T*)	AYE
RS40	$CH_3SO_3 + HCHO \rightarrow MSA + HO_2 + CO$	1.6E-15	YIN
RS41	$CH_3SO_3 + DMS \rightarrow MSA + CH_3SCH_2$	6.8E-14	YIN
RS42	$CH_3SO_3 + HO_2 \rightarrow MSA$	5.E-11	YIN
RS43	$CH_3SO_3 + H_2O_2 \rightarrow MSA + HO_2$	3.E-16	YIN

Table 2. (continued)

	Reaction	Rate	Reference
	SO_2 Chemistry		
RS44	$SO_2 + OH \rightarrow HSO_3$	(2)	YIN
RS45	$SO_2 + HO_2 \rightarrow SO_3 + OH$	1.E-18	YIN
RS46	$SO_2 + CH_3O_2 \rightarrow HCHO + HO_2 + SO_3$	5.E-17	YIN
RS47	$HSO_3 + O_2 \rightarrow SO_3 + HO_2$	1.0E-11 x exp(-1000/ *T*)	YIN
RS48	$SO_3 + H_2O \rightarrow$ H2SO4B	9.1E-13	YIN
RS49	$SO_2 + O_3 \rightarrow$ PROD1	3.E-12 x exp(-7000/ *T*)	YVO96
	SO_2 Heterogeneous Oxidation		
RS50	SO_2 (incloud) $\rightarrow H_2SO_4B$	1.1E-6	YVO96
RS51	SO_2 (on sea-salt) $\rightarrow H_2SO_4P$	8.3E-5	[*Krischke et al.*, this issue]
	SO Chemistry		
RS52	$SO + O_2 \rightarrow SO_2 + O$	1.4E-13 x exp(-4.52/0.0019872/ *T*)	YIN
RS53	$SO + NO_2 \rightarrow SO_2 + NO$	1.4E-11	YIN
RS54	$SO + O_3 \rightarrow SO_2 + O_2$	1.8E-15 x exp(-2.33/0.0019872/ *T*)	YIN
RS55	$SO + OH \rightarrow SO_2 + HO_2$	1.1E-10	YIN

Note: *T* is air temperature in kelvins. [a] Read 1.1E-11 as 1.13×10^{-11}. [b] Not included in the basic simulation. (1) ROHDMSA= RX1/RX2, where RX1= 1.7E-42 x exp(7810/*T*) x AIR x 0.2197 and RX2=1+5.5E-31 x exp(7460/*T*) x AIR x 0.2197. (2) $ROHSO_2$= RX1/(1. + RX1/RX2) x (0.5)(1./(1. + [LOG10(RX1/RX2)]^2)), where RX1= 3.0E-31 x $(T/300)^{-3.3}$ x AIR and RX2= 1.5E-12. References : JPL97, *De More et al.* [1997]; KT96, *Koga and Takana* [1996]; CRO99, *Ingham et al.*, [1999]; YIN, *Yin et al.* [1990]; AYE, *Ayers et al.* [1996]; YVO96, *Yvon and Saltzman* [1996]; CP 97, *Capaldo and Pandis* [1997].

the oxidation chemistry of NMHC including biogenic hydrocarbons and sulfur compounds. The C_1-C_5 hydrocarbon chemistry in this scheme has been validated against a detailed chemistry scheme (about 10,000 reactions [*Poisson*, 1997; *Poisson et al.*, 1999]) and is also used in a global three-dimensional model [*Kanakidou and Crutzen*, 1999].

3.6.2.1. DMS oxidation chemistry: For the present study, this scheme has been complemented to describe DMS oxidation chemistry initiated by OH radicals. The adopted DMS chemistry is presented in Table 2 and is structured following the DMS oxidation scheme published by *Yin et al.* [1990] and reduced as suggested by *Capaldo and Pandis* [1997]. For SO_2, in-cloud oxidation occurs with a pseudo first-order rate of 1.1×10^{-6} s^{-1}, whereas for its loss on sea-salt aerosols the value of 8.3×10^{-5} s^{-1} has been adopted (calculated from the second order constant estimated by *Krischke et al.* [this issue] during this cruise, and the particle number during these days).

The temperature-dependent rates of decomposition of CH_3SO_2 and CH_3SO_3, estimated by *Ayers et al.* [1996] following the laboratory observations by *Good and Thynne* [1967] and *Turnipseed and Ravishankara* [1993], replaced the recommended by *Yin et al.* [1990] values.

3.6.2.2. Physical processes: A constant sea-to-air flux of DMS of 4.0±0.9 μmol m^{-2} d^{-1}, experimentally calculated during this work, has been used in the model for the studied 2-day period. These emissions are assumed to be uniformly distributed in the mixed layer of 550 m and thus correspond to a production rate for DMS of $6.34\ 10^4$ molecules cm^{-3} s^{-1}.

Vertical entrainment of air from the free troposphere to the mixed layer is also taken into account. This air is assumed to contain no sulfur compounds. An entrainment velocity of 0.168 cm/s is adopted for DMS, MSA and H_2SO_4, as suggested by *Yvon et al.* [1996] and in agreement with the range of 0.1 to 0.5 cm/s suggested by *Lenschow et al.* [1988]. In our model this correspond to a pseudo first-order loss rate of $3.05\ 10^{-6}$ s^{-1}.

Dry deposition V_d, which is species specific, is taken into account in the model. In particular, deposition velocities have been used for DMSO and $DMSO_2$ (0.5 cm/s), MSA and fine SO_4 (0.1 cm/s), and for large SO_4 particles (produced in our model by heterogeneous reactions of SO_2 on sea-salt particles: 0.7 cm/s). For SO_2 the empirical formula relating V_d and wind speed U proposed by *Yvon et al.* [1996] ($V_d = 1.2\ 10^{-3} \times U$) is used.

3.6.2.3. Input parameters: Hourly mean observations of H_2O, pressure, temperature, photolysis frequencies of NO_2 (JNO_2) and O_3 to O^1D (JO^1D), O_3, NO, NO_2, CO, C_2H_6, C_2H_4, C_3H_8, H_2O_2, and HCHO were used as input to the box model every hour. Thus physical processes (emissions, deposition, transport) important for such relatively long-lived species are taken into account every hour in our box models. This approach would not be valid if transport processes were sufficiently rapid. In this case dilution would impact on the behavior of short-lived species. Indeed, this did not occur during the studied 2 days since no significant changes in the origin of sampled air masses took place that period. HNO_3 concentrations were fixed to 10 pptv at the beginning of the simulations, which corresponds to the observed mean value over that period. CH_4 concentrations were fixed to 1.8 ppmv at the beginning of the simulations. The photolysis rates of reactions other than photodissociation of O_3 to $O(^1D)$ and NO_2, were calculated by a radiative transfer model using the two stream method [*Brühl and Crutzen*, 1988]. The model results were adjusted to reproduce the measured photolysis frequencies of NO_2 and O_3.

3.6.2.4. Scenarios: To investigate the importance of OH radical in DMS oxidation the first simulation of DMS diurnal cycle has been performed with DMS chemistry scheme as shown in Table 2 but neglecting the reaction of DMS with

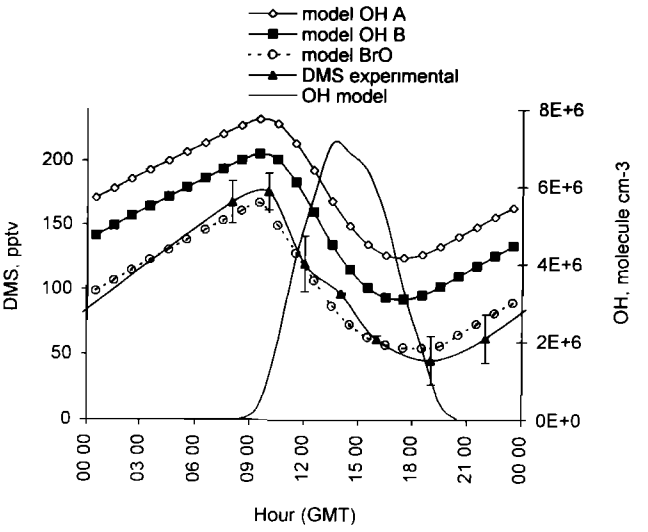

Figure 7. Comparison between the model results and the DMS observations during the Albatross cruise and for the period October 25-26, 1996.

BrO. For this first simulation (reported as "OH A" in Figure 7), the rate of the OH addition and H abstraction pathways of DMS with OH reaction are taken from *Atkinson et al.* [1997] recommendations. A second simulation (reported as "OH B" in Figure 7) has been performed as above but by increasing the reaction rates of DMS with OH by 30% to fit the laboratory measurements by *Barnes et al.* [1996]. Finally, a third simulation (reported as "BrO" in Figure 7) has been performed by using the *Atkinson et al.* [1997] reaction rates and taking into account the depletion of DMS by BrO assuming that this reaction leads by 100% to DMSO [*Ingham et al.*, 1999]. For this simulation a constant BrO concentration of 3 pptv has been used during the day from 0900 UT to 1800 UT. This value is almost 2 times higher than the model estimates by *Vogt et al.* [1999]. It is, however, close to the lower end of 4-17 pptv observed by *Hausmann and Platt* [1993] in the Arctic boundary layer air in spring and much lower than the observations by *Hebestreit et al.* [1999] at mid latitudes, where high values of BrO up to 80 pptv where measured. All three simulations have been performed twice: once by adopting the mean DMS sea-to-air flux calculated experimentally during this cruise of 4 μmol m^{-2} d^{-1} and a second time by adopting the upper limit of our DMS flux of 5 μmol m^{-2} d^{-1}.

3.6.3. Chemical model results and discussion. When adopting the mean DMS flux of 4 μmol m^{-2} d^{-1} in our model, the calculated evening recovery of DMS, which is modulated by the sea-to-air flux of DMS and starts when its chemical sink becomes negligible, is rather slow compared to the observations. A sharper recovery of DMS during the evening hours, similar to that observed, is simulated when adopting the upper limit of the experimentally calculated DMS sea-to-air flux. Therefore only the second set of simulations, using DMS flux of 5 μmol m^{-2} d^{-1} will be further presented and discussed.

The simulated mean diurnal variations of DMS for the three scenarios are shown in Figure 7 and compared with observations. Focusing on the two first simulations named "OH A" and "OH B". It is obvious that for both scenarios the DMS simulated concentrations are significantly higher than the observations. Similar results have been obtained by *Yvon et al.* [1996], who pointed out the need of an increase of the photochemical oxidation rate of DMS by a factor of 2 to reproduce the observed atmospheric DMS diurnal cycle. On the other hand, the chemical model is able to approximately simulate the diurnal trend of DMS with a maximum in the morning hours and a minimum in the afternoon. However, the DMS recovery, that occurs in the evening when the chemical sink of DMS becomes very weak starts earlier in the simulation. It appears that the chemical sink of DMS in the model is rather weak by the end of the afternoon. In the model this sink is occurring by reaction with OH radical. In addition, the simulated by the model OH radical diurnal distribution agrees remarkably well with the observed OH radical levels (T. Brauers et al., unpublished manuscript, 1999). Note that uncertainties in the DMS flux calculation are at least of a factor of 2. In our simulation DMS flux has been calculated using the *Liss and Merlivat* [1986] parameterization. The use of one of the other two existent parameterizations for DMS flux calculation, that is, that proposed by *Smethie et al.* [1985] or *Wanninkhof* [1992], resulted in a DMS flux higher by a factor of 1.25 to 1.6 to our input value, respectively. Such high DMS fluxes are not consistent with our DMS measurements since it would increase more the simulated DMS concentrations.

A possible explanation for the discrepancy between model results and observations is that other radicals like BrO might significantly contribute to the DMS sink and particularly to the morning and late afternoon DMS depletion. Indeed, according to model calculations by *Toumi* [1994] and *Vogt et al.* [1999], BrO radicals are expected to present a diurnal pattern different from that of OH, increasing sharply in the morning, decreasing very sharply by the end of the day and in between showing a local minimum. Such a diurnal profile could correspond to the missing afternoon sink of DMS. Indeed, when assuming that BrO is present in the marine

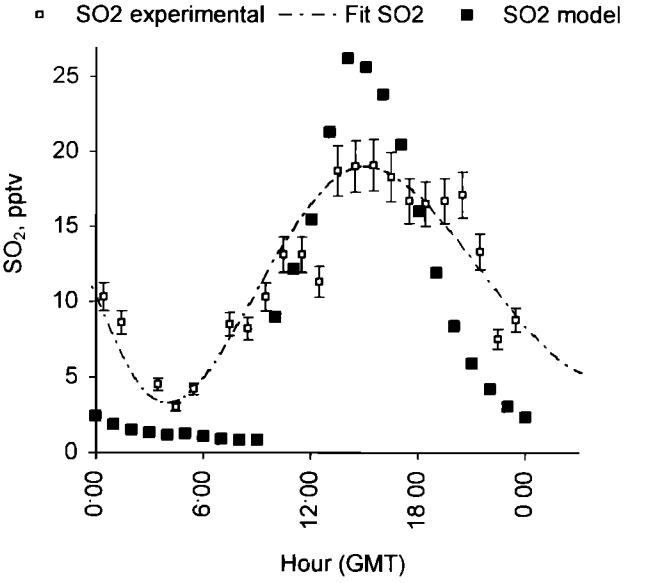

Figure 8. Comparison between the model results and the SO_2 observations during the Albatross cruise and for the period October 25-26, 1996.

mixed layer in levels of 3 pptv during day, a very good agreement is obtained between the computed and observed DMS concentrations. BrO radicals account for a reduction of roughly 30% in the DMS morning concentrations and of about 60% in the late afternoon values. Consideration of DMS oxidation by BrO leads also to a shift in the timing of the afternoon minimum in DMS toward late afternoon and fits that better with observations.

In Figure 8, the measured SO_2 concentrations are compared with the model results. In general, the model reproduces well a daytime maximum and an evening minimum in agreement with observations. Note that the model simulates lower values during nighttime compared than the observations that are very close to the detection limit of the method (3.6 pptv).

On the basis of the DMS observations and to fit the SO_2 values observed by *Krischke et al.* [this issue], a total conversion factor (SO_2 production/ DMS destruction) of 0.39 is calculated by our chemical model. For this the total oxidation of DMS (by OH and BrO radicals) and the production of SO_2 by the reaction of DMS with OH radical were taking into account. This factor is higher than the estimate of 27% for the total conversion of DMS to SO_2 calculated by *Yvon et al.* [1996]. Note that for our calculations the oxidation of DMS by BrO is assumed to lead to unknown products as shown in Table 2, thus not affecting SO_2 levels. The reason for this is the lack of sufficient knowledge on the fate of DMSO, the expected main oxidation product of DMS reaction with BrO in the marine atmosphere. Note that DMSO is also produced by DMS reaction with OH. However, its yield for the temperatures encountered during our cruise is very low (about 10%) and thus, under the studied experimental conditions, it has very little influence on the SO_2 production.

When considering the depletion of DMS by OH radical alone, we calculate, as expected, a higher conversion rate of DMS to SO_2 of 0.8. This value reasonably compares with the 0.62±0.06 calculated by *Bandy et al.* [1996] and the 0.60-0.80 estimated by *De Bruyn et al.* [1998] for the tropical atmosphere. It is somewhat higher than the 54% conversion of DMS to SO_2 by the reaction with OH radicals given by *Yvon et al.* [1996]. The calculated particulate nss-SO_4 of 106 ± 11 pptv is in good agreement with the observed diurnal mean value of 108 ± 12 pptv.

4. Conclusions

Measurements of atmospheric DMS and its oxidation products SO_2, nss-SO_4, MSA, and DMSOp were made during the Albatross cruise aboard the R/V *Polarstern* in the Atlantic Ocean in October and November 1996.

DMSOp observations in aerosols and its size distribution have been reported for the first time in our knowledge in the marine atmosphere of the Atlantic Ocean. Its spatial variation in particles sized less than 0.44 μm follows the general trend of F_{DMS}, suggesting that DMSOp is produced from local sources of DMS and has a relatively short lifetime compared with those of MSA and nss-SO_4.

Long-range transport, local sea-to-air flux of DMS (F_{DMS}), MBL height variation, and photochemistry were found to be the major factors controlling atmospheric DMS concentration. The amplitude of the daytime cycle in atmospheric DMS is significantly larger than that predicted by a photochemical model when reaction with OH radical is the only considered sink for DMS. Since simultaneous measurements of MBL height, OH in the atmosphere, and DMS in the seawater exist, the only way to reconcile the model with the observations is to increase the photochemical oxidation rate of DMS by about 30%-60%. BrO at concentrations of the order of 2-3 pptv can reproduce the observed daytime cycle in atmospheric DMS. Moreover, according to the chemical model results, DMS oxidation is the dominant source of SO_2 in the equatorial unpolluted region.

Acknowledgments. We would like to thank T. Brauers and H.P. Dorn for providing OH and CN data, A. Gogou for help in sampling, T. Savidis and H. Nezis for their help in analysis, and three anonymous reviewers for their constructive comments. This work has been supported by the EU-MARATHON program ENV4-CT95-0004.

References

Andreae, M.O., Determination of trace quantities of dimethylsulfoxide in aqueous solutions, *Anal. Chem., 52*, 150-153., 1980.

Andreae, M.O., R.J. Ferek, F. Bermond, K.P. Byrd, R.T. Engstrom, S. Hardin, D. Houmere, F. LeMarrec, H. Raemdonck, and R.B. Chatfield, Dimethylsulfide in the marine atmosphere, *J. Geophys. Res., 90*, 12,891-12,900, 1985.

Andreae, M.O., W. Elbert, and S.J. de Mora, Biogenic sulfur emissions and aerosols over the tropical South Atlantic, 3, Atmospheric dimethylsulfide, aerosols, and cloud condensation nuclei, *J. Geophys. Res., 100*, 11,335- 11,356, 1995.

Atkinson, R., D. L. Baulch, R.A. Cox, R.F. Hampson Jr., J. A. Kerr, M. J. Rossi, and J. Troe, Evaluated kinetic and photochemical data for atmospheric chemistry: Supplement VI, IUPAC subcommittee on gas kinetic data evaluation for atmospheric chemistry, *J. Phys. Chem. Ref. Data, 26*, 1329-1499, 1997.

Ayers, G.P., S.T. Bentley, J.P. Ivey, and B.W. Forgan, Dimethylsulfide in marine air at Cape Grim, 41°S, *J. Geophys. Res., 100*, 21,013-21,021, 1995.

Ayers, G.P., J.M. Cainey, H. Granek, and C. Leck, Dimethylsufide oxidation and the ratio of methanesulfonate to non sea-salt sulfate in the marine aerosol, *J. Atmos. Chem.*, *25*, 307-325, 1996.

Ayers, G.P., J.M. Gainey, R.W. Gillet, E.S. Saltzman, and M. Hopper, Sulfur dioxide and dimethylsulfide in the marine air at Cape Grim, 41°S, *Tellus, Ser. B., 49*, 292-299, 1997.

Baboukas, E. D., M. Kanakidou, N. Mihalopoulos and R. Weller, Carboxylic acids in gas and particulate phase above the Atlantic Ocean, *J. Geophys. Res.*, this issue.

Bandy, A.R., D.C. Thornton, B.W. Blomquist, S. Chen, T.P. Wade, J.C. Ianni, G.M. Mitchell, and W. Nadler, Chemistry of dimethyl sulfide in the equatorial Pacific atmosphere, *Geophy. Res. Lett., 23*, 741-744, 1996.

Barnes, I., K.H. Becker, and I. Patroescu, FTIR products study of the OH initiated oxidation of dimethyl sulphide: Observation of carbonyl sulphide and dimethyl sulphoxide, *Atmos. Environ., 30*, 1805-1814, 1996.

Bates, T.S., J.A. Calhoun, and P.K. Quinn, Variations in the methanesulfonate to sulfate molar ratio in submicrometer marine aerosol particles over the South Pacific Ocean, *J. Geophys. Res., 97*, 9859-9865, 1992.

Bates, T. S., B. J. Huebert, J. L. Gras, F. B. Griffiths, and P.A. Durkee, International Global Atmospheric Chemistry (IGAC) Project's First Aerosol Characterization Experiment (ACE 1): Overview, *J. Geophys. Res., 103*, 16,297-16318, 1998.

Belviso, S., R. Morrow, and N. Mihalopoulos, An Atlantic meridional transect of surface water DMS concentrations with 10-15 km horizontal resolution and close examination of ocean circulation, *J. Geophys. Res.*, this issue.

Brühl, C., and P.J. Crutzen, Scenarios of possible change in atmospheric temperatures and ozone concentrations due to man's activities, estimated with a one-dimensional coupled photochemical climate model, *Clim. Dyn.*, 2, 173-203, 1988.

Bürgermeister, S., and H.-W. Georgii, Distribution of methanesulfonate, nss sulfate and dimethylsulfide over the

Atlantic and the North Sea , *Atmos. Environ., Part A, 25* (3-4), 587-595, 1991.

Capaldo, K., and S. Pandis, Dimethylsulfide chemistry in the remote marine atmosphere: Evaluation and sensitivity analysis of available mechanisms, *J. Geophys. Res., 102,* 23,251-23,267, 1997.

Charlson, R.J., J. Lovelok, M.O. Andreae, and S. Warner, Oceanic phytoplankton, atmospheric sulfur, cloud albedo and climate, *Nature, 326,* 655, 1987.

Chin, M., D. J. Jacob, G. M. Gardner, M. S. Foreman-Fowler, P.A.. Spiro, and D.L. Savoie, A global three-dimensional model of tropospheric sulfate, *J. Geophys. Res., 101,* 18,667-18,691, 1996.

Curtis, A., and W. Sweetenham, FACSIMILE/CHEKMAT users manual, *AERE-R12805,* Harwell Lab., Oxfordshire, England, 1988.

Davis, D., G. Chen, P. Kasibhatla, A. Jefferson, D. Tanner, F. Eisele, D. Lenschow, W. Neff, and H. Berresheim, DMS oxidation in the Antarctic marine boundary layer: Comparison of model simulations and field observations of DMS, $DMSO_2$, H_2SO_4 (g), MSA (g), and MSA (p), *J. Geophys. Res., 103,* 1657-1678, 1998.

Davison, B., C. N. Hewitt, C.D. O'Dowd, J.A. Lowe, M.H. Smith, M. Schwikowski, U. Baltensperger, and R.M. Harrison, Dimethyl sulfide, methane sulfonic acid, and physicochemical aerosol properties in Atlantic air from the United Kingdom to Halley Bay, *J. Geophys. Res., 101,* 22,855-22,867, 1996.

De Bruyn, W., T.S. Bates, J.M. Gainey, and E. Saltzman, Shipboard measurements of dimethyl sulfide and SO_2 southwest of Tasmania during the First Aerosol Characterization Experiment (ACE 1), *J. Geophys. Res. , 103,* 16,703-16,711, 1998.

DeMore, W. B., S.P. Sander, D. Golden, R. F. Hampson, M.J. Kurylo, C. J. Howard, A. R. Ravishankara, C.E. Kolb, and M.J. Molina, Chemical kinetics and photochemical data for use in stratospheric modeling: Evaluation n°12, *JPL Publ., 97-4,* 1997.

Galloway, J.N., D.L. Savoie, W. Keene, and J.M. Prospero, The temporal and spatial variability of scavenging ratios for nss-SO_4, nitrate, methanesulfonate and sodium in the atmosphere over the North Atlantic Ocean, *Atmos. Environ., 27,* 235-250, 1993.

Good, A., and J.C.J. Thynne, Reactions of free radicals with sulphur dioxide, *J. Chem. Soc. Faraday Trans., 63,* 2708-2719, 1967.

Hausmann, M., and U. Platt, BrO measurements in the high Arctic, *Ann. Geophys., 11,* suppl. 3, C416, 1993.

Hebestreit, K., J. Stutz, D. Rosen, V. Matveev, M. Peleg, M. Luria, and U. Platt, First DOAS measurements of tropospheric BrO in mid latitudes, *Science, 283,* 55-57, 1999.

Herman, J., and W. Jaeschke, Measurements of H_2S and SO_2 over the Atlantic Ocean, *J. Atmos. Chem., 1,* 111-123, 1984.

Huebert, B.J., D.J. Wylie, L. Zhuang, and J. A. Heath, Production and loss of methanesulfonate and non-sea-salt sulfate in the equatorial Pacific marine boundary layer, *Geophys. Res. Lett., 23,* 737-740, 1996.

Hynes, A.J., and P.H. Wine, The atmospheric chemistry of dimethylsulfoxide (DMSO) kinetics and mechanism of the OH + DMSO reaction, *J. Atmos. Chem., 24,* 23-37, 1996.

Ingham, T., D. Brauer, R. Sander, P.J. Crutzen, and J.N. Crowley, Kinetics and products of the reaction BrO + DMS and Br + DMS, *J. Phys. Chem., 103,* 7199-7209, 1999.

Intergovernmental Panel on Climate Change (IPCC), *Climate Change 1994,* edited by J. Houghton and G. Meira, Cambridge Univ. Press, New York, 1994.

Kanakidou, M., and P.J. Crutzen, The photochemical source of carbon monoxide: Importance, uncertainties and feedbacks, *Chemosphere Global Change Sci., 1,* 91-109, 1999.

Kieber, M.D., J. Jiao, R.P. Kiene, and T.S. Bates, Impact of dimethyl sulfide production on methyl sulfur cycling in the equatorial Pacific Ocean, *J. Geophys. Res., 101,* 3715-3722, 1996.

Koga, S., and H. Takana, Simulations of seasonal variations of sulfur compounds in the remote marine atmosphere, *J. Atmos. Chem., 23,* 163-192, 1996.

Krischke U., R. Staubes, T. Brauers, M. Gautrois, J. Burkert, D. Stöbener, and W. Jaeschke, Removal of SO_2 from the marine boundary layer over the Atlantic Ocean: A case study on the kinetics of the heterogeneous S(IV) oxidation on marine aerosols, *J. Geophys. Res.,* this issue.

Lawrence, J. E. , and P. Koutrakis, Measurement of atmospheric formic and acetic acids: Methods evaluation and results from field studies, *Environ. Sci. Technol., 28,* 957-964, 1994.

Lenschow, D.H., I.R. Paulch, A.R. Bandy, R. Pearson Jr, S.R. Kawa, C.J. Weaver, B.J. Huebert, J.G. Kay, D.C. Thorton, and A.R. Drieger III, Dynamics and Chemistry of Marine Stratocumulus Experiment (DYCOMS) experiment, *Bull. Am. Meteorol. Of Soc., 69,* 1058-1067, 1988.

Liss, P.S., and L. Merlivat, *The Role of Air-Sea Exchange in Geochemical Cycling,* edited by P. Buat-Ménard, pp. 113-127, D. Reidel , Norwell, Mass., 1986.

Liss, P.S. and P.G. Slater, Flux of gases across the air-sea interface. *Nature, 247,* 181-184, 1974.

Nguyen, B.C., B. Bonsang, and A. Gaudry, The role of the ocean in the global atmospheric sulfur cycle, *J. Geophys. Res., 88,* 10,903-10,914, 1983.

Nguyen, B.C., N. Mihalopoulos, and S. Belviso, Seasonal variation of atmospheric dimethylsulfide at Amsterdam Island in the southern Indian Ocean, *J. Atmos. Chem., 11,* 123-143, 1990.

Patris, N., N. Mihalopoulos, E. Baboukas, and J. Jouzel, Isotopic composition of sulfur in size-resolved marine aerosols above the Atlantic Ocean, *J. Geophys. Res.,* this issue.

Poisson, N., Impact des hydrocarbures non méthaniques sur la chimie troposphérique, Ph.D. thesis, pp. 253, Univ. Paris 7, Paris, France, 1997.

Poisson, N., et al., The impact of natural nonmethane hydrocarbon oxidation on the free radical and ozone budgets above a eucalyptus forest, *Chemosphere,* in press, 2000.

Putaud, J.P., S. Belviso, B.C. Nguyen, and N. Mihalopoulos, Dimethylsulfide, aerosols, and condensation nuclei over the tropical northeastern Atlantic Ocean, *J. Geophys. Res., 98,* 14,863-14,871, 1993.

Sciare J. and N. Mihalopoulos, A new technique for sampling and analysis of atmospheric dimethylsulfoxyde (DMSO), *Atmos. Environ., 34,* 151-156, 2000.

Sciare, J., E. Baboukas, R. Hancy, N. Mihalopoulos, and B.C. Nguyen, Seasonal variation of dimethylsulfoxide (DMSO) in rainwater at Amsterdam Island in the southern Indian Ocean: Implications on the biogenic sulfur cycle, *J. Atm. Chem., 30,* 229-240, 1998.

Simo, R., J. O. Grimalt, and J. Albaiges, Dissolved dimethyl-sulphide, dimethyl-sulfoniopropionate and dimethylsulfoxide in western Mediterranean waters, *Deep Sea Res., Part II, 44,* 929-950, 1997.

Smethie, W. M., Jr., T. Takahashi, D. W. Chipman, and J.R. Ledwell, Gas exchange and CO_2 flux in the tropical Atlantic Ocean determined from ^{222}Rn and pCO_2 measurements, *J. Geophys. Res., 90,* 7005-7022, 1985.

Staubes, R., and H.-W. Georgii, Measurements of atmospheric and seawater DMS concentrations in the Atlantic, the Arctic and Antarctic region, in *Dimethylsulphide: Oceans, Atmosphere, and Climate,* edited by G. Restelli and G. Angeletti, pp. 95-102, Kluwer Acad., Norwell, Mass., 1993.

Toumi, R., BrO as a sink for dimethylsulfide in the marine atmosphere, *Geophys. Res. Lett., 21,* 117-120, 1994.

Turnipseed, A.A., and A.R. Ravishankara, The atmospheric oxidation of dimethylsulfide: Elementary steps in a complex mechanism, in *Dimethylsulphide: Oceans, Atmosphere, and Climate,* edited by G. Restelli and G. Angeletti, pp. 185-195, Kluwer Acad., Norwell, Mass., 1993.

Vogt, R., R. Sander, R. Von Glasow and P.J. Crutzen, Iodine chemistry and its role in halogen activation and ozone loss in the marine boundary layer: A model study, *J. Atm. Chem., 32,* 375-395, 1999.

Wanninkhof, R., Relationship between gas exchange and wind speed over the ocean, *J. Geophys. Res., 97,* 7373-7381, 1992.

Watts, S.F., P. Brimblecomble, and A. Watson, Methanesulphonic acid, dimethyl sulfoxide and dimethyl sulphone in aerosols, *Atmos. Environ., Part A, 24,* 353-359, 1990.

Yin, F., D. Grosjean, and J.H. Seinfeld, Photooxidation of dimethylsulfide and dimethyldisulfide: Mechanism development, *J. Atm. Chem., 11,* 309-364, 1990.

Yvon, S.A., and E. S. Saltzman, Atmospheric sulfur cycling in the tropical Pacific marine boundary layer (12°S, 135°W): A comparison of field data and model results, 2, Sulfur dioxide, *J. Geophys. Res., 101,* 6911-6918, 1996.

Yvon, S.A., E. S. Saltzman, D.J. Cooper, T.S. Bates, and A.M. Thompson, Atmospheric sulfur cycling in the tropical Pacific

marine boundary layer (12°S, 135°W): A comparison of field data and model results, 1, Dimethylsulfide, *J. Geophys. Res., 101*, 6899-6909, 1996.

E. Baboukas, H. Bardouki, M. Kanakidou, and N. Mihalopoulos (corresponding author), Environmental Chemical Processes Laboratory, Department of Chemistry, University of Crete, P.O. Box 1470, 71409 Heraklion, Greece (mariak@chemistry.uch.gr, mihalo@chemistry.uch.gr).

S. Belviso and J. Sciare, Laboratoire des Sciences du Climat et de l'Environnement, CEA Orme des Merisiers, 91191 Gif-Yvette Cedex, France (sciare@lsce.saclay.cea.fr).

U. Krischke, Department of Atmospheric Sciences, UCLA, Los Angeles, CA 90095-1565.

(Received June 25, 1999; revised November 22, 1999 ; accepted November 30, 1999.)